

Functional Differences in Epigenetic Modulators—Superiority of Mercaptoacetamide-Based Histone Deacetylase Inhibitors Relative to Hydroxamates in Cortical Neuron Neuroprotection Studies

Alan P. Kozikowski,^{*,†} Yufeng Chen,[†] Arsen Gaysin,[†] Bin Chen,[†] Melissa A. D'Annibale,[‡] Carla M. Suto,[§] and Brett C. Langley^{‡,||}

Drug Discovery Program, Department of Medicinal Chemistry and Pharmacognosy, University of Illinois at Chicago, 833 South Wood Street, Chicago, Illinois 60612, Burke Medical Research Institute, White Plains, New York 10605, Amphora Discovery Corporation, 800 Capitola Drive, Durham, North Carolina 27713, and Department of Neurology and Neuroscience, Weill Medical College of Cornell University, New York, New York 10021

Received February 15, 2007

We compare the ability of two structurally different classes of epigenetic modulators, namely, histone deacetylase (HDAC) inhibitors containing either a hydroxamate or a mercaptoacetamide as the zinc binding group, to protect cortical neurons in culture from oxidative stress-induced death. This study reveals that some of the mercaptoacetamide-based HDAC inhibitors are fully protective, whereas the hydroxamates show toxicity at higher concentrations. Our present results appear to be consistent with the possibility that the mercaptoacetamide-based HDAC inhibitors interact with a different subset of the HDAC isozymes [less activity at HDAC1 and 2 correlates with less inhibitor toxicity], or alternatively, are interacting selectively with only the cytoplasmic HDACs that are crucial for protection from oxidative stress.

Introduction

To date, considerable research activity has focused on understanding the “histone code” and, in particular, on the design of histone deacetylase (HDAC^a) inhibitors as novel therapeutics for the treatment of a wide range of disorders including cancer, as well as neurodegenerative diseases, and even malaria.¹ These compounds owe their action to their ability to reactivate silenced genes by modulating the condensation status of DNA. The post-translational acetylation status of chromatin is determined by the competing activities of two classes of enzymes, histone acetyltransferases (HATs) and HDACs, which control the acetylation of lysine residues making up the histones. In general, HATs function to acetylate lysine groups in nuclear histones, resulting in neutralization of the charges on the histones and a more open, transcriptionally active chromatin structure, while the HDACs function to deacetylate and suppress transcription. A shift in the balance of acetylation on chromatin may result in changes in the regulation of patterns of gene expression.^{2–5} Because many cancers are associated with aberrant transcriptional activity and HDACs can affect transcription factors and gene regulation, these enzymes have been identified as attractive targets for cancer therapy. Indeed, chemical inhibitors of HDACs have been shown to inhibit tumor cell growth and induce differentiation and cell death.⁶ Several such inhibitory agents, including suberoylanilide hydroxamic acid (SAHA) and depsipeptide (FR901228) have reached clinical trials,^{7–9} and SAHA has been approved by the FDA for use in cutaneous T-cell lymphoma (CTCL). HDAC inhibitors work by allowing the

transcription and expression of genes, including tumor suppressor genes. HDAC inhibitors also enhance the cytotoxic effects of therapeutic agents used in cancer treatment, including radiation and chemotherapeutic drugs.^{10,11}

In addition to their applications in oncology, several of the known HDAC inhibitors have been found to be protective in different cellular and animal models of acute and chronic neurodegenerative injury and disease, for example, ischemic stroke,^{12–14} multiple sclerosis,¹⁵ and polyglutamine-expansion diseases, such as Huntington's disease^{16–20} and spinal and bulbar muscular atrophy (SBMA).²¹ Thus, the administration of SAHA in drinking water using cyclodextrin as a carrier and sodium butyrate administered intraperitoneally have been shown to significantly improve rotarod performance and to decrease neuronal atrophy in R6/2 mice. Sodium butyrate treatment significantly extended survival in R6/2 mice by 20%. Consistent with the idea that HDAC inhibition relieves transcriptional repression and that protection is downstream of mutant htt, neither inhibitor was found to decrease mutant htt expression or aggregates.¹⁷ The use of sodium butyrate as a therapy has also been explored in a transgenic mouse model of SBMA. Oral administration of this compound increased histone acetylation in spinal cord tissue and was found to reduce the functional and histopathological deficits associated with SBMA. Moreover, Nestler has recently highlighted the therapeutic potential of HDAC inhibitors (HDAC5) in depression.²²

The utility of HDAC inhibitors in medicine would thus appear to be tremendous, but the translation of these ideas to the clinic will ultimately require the design of isoform selective molecules to minimize side effect issues. The HDAC inhibitors now in the clinic do not show any significant selectivity for the individual HDAC isoforms of which there are now 11 that operate by zinc (or possibly iron²³) dependent mechanisms (class I includes HDACs 1, 2, 3, and 8, class II includes 4, 5, 6, 7, 9, and 10, and class IV includes HDAC 11).^{24,25} While we were still investigating complete details of isoform selectivity of our designed HDAC inhibitors, we deemed it important to examine

* To whom correspondence should be addressed. Phone: 312-996-7577. Fax: 312-996-7107. E-mail: kozikowa@uic.edu.

[†] University of Illinois at Chicago.

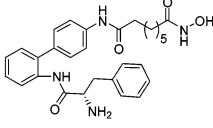
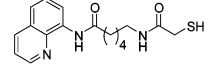
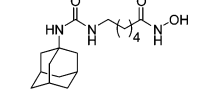
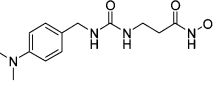
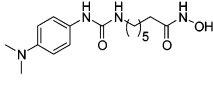
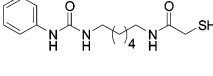
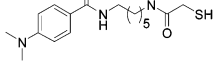
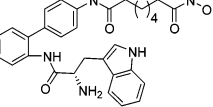
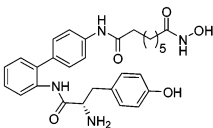
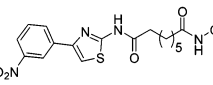
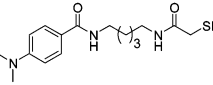
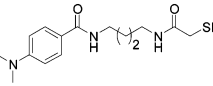
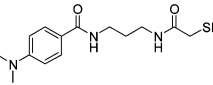
[‡] Burke Medical Research Institute.

[§] Amphora Discovery Corporation.

^{||} Weill Medical College of Cornell University.

^a Abbreviations: HDAC, histone deacetylase; ZBG, zinc binding group; HAT, histone acetyltransferase; SAHA, suberoylanilide hydroxamic acid; TSA, trichostatin A; CTCL, cutaneous T-cell lymphoma; SBMA, spinal and bulbar muscular atrophy; HCA, homocysteate; MTT, 3-[4,5-dimethylthiazol-2-yl]2,5-diphenyltetrazolium bromide.

Table 1. List of Compounds Studied in the Neuroprotection Assays Using Cortical Neurons

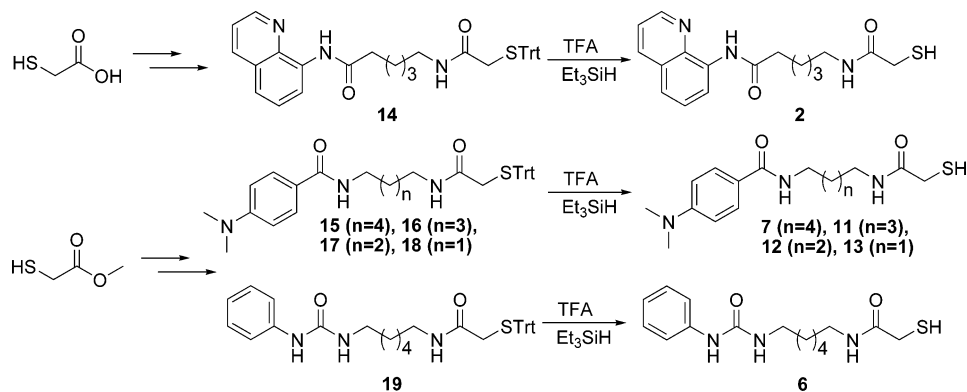
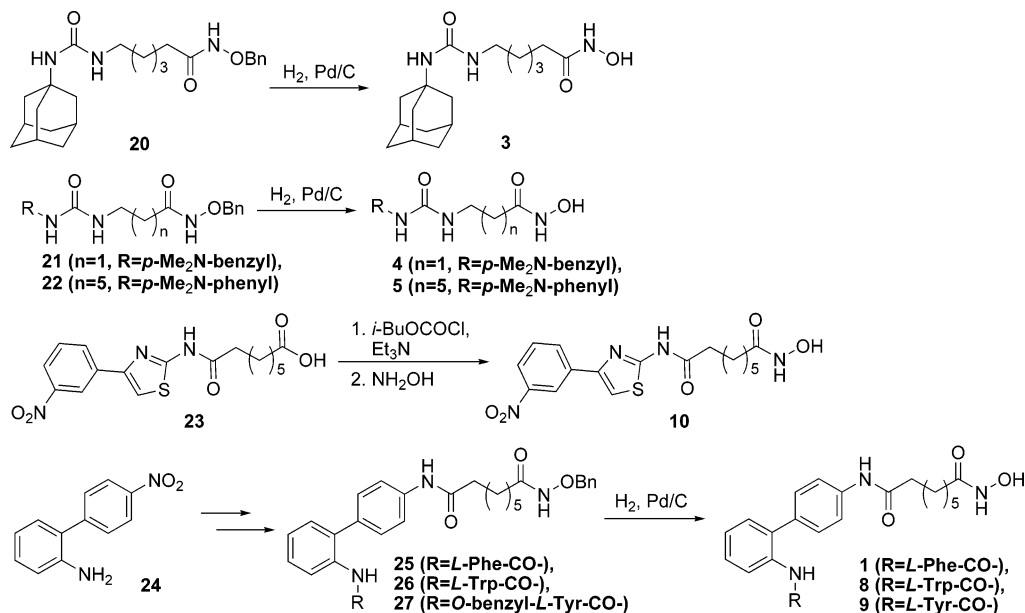
Compd	Structure	CLogP (KowWin) ^a	IC ₅₀ (nM) values against HDAC isoforms				
			HDAC1	HDAC2	HDAC8	HDAC10	HDAC6
1		2.80	40.9 ± 4.0	156 ± 5	1600 ± 60	46.1 ± 4.4	7.5 ± 0.5
2		2.43	3220 ± 190	7380 ± 300	6120 ± 40	10700 ± 1800	95.3 ± 1.3
3		2.29	152 ± 6	1050 ± 30	3410 ± 20	173 ± 16	102 ± 1
4		2.09	130 ± 10	492 ± 9	1050 ± 20	178 ± 21	45.5 ± 0.6
5		1.69	209 ± 22	647 ± 43	1740 ± 80	176 ± 32	34.5 ± 0.8
6		2.04	10800 ± 1800	>30000	13900 ± 600	>30000	2010 ± 60
7		2.25	1430 ± 130	4640 ± 320	19100 ^b	3430 ± 490	482 ± 16
8		2.86	26.7 ± 1.8	167 ± 12	1720 ± 70	28.3 ± 3.9	5.4 ± 0.4
9		2.32	36.9 ± 2.6	205 ± 10	2060 ± 80	42.1 ± 4.0	9.0 ± 0.6
10		2.77	8.5 ± 0.6	113 ± 6	4090 ± 330	11.1 ± 1.3	3.7 ± 0.2
11		1.76	1080 ± 70	6460 ± 570	10200 ± 500	1540 ± 390	114 ± 6
12		1.27	11900 ± 1100	>30000	>30000	29700 ± 13500	620 ± 15
13		0.78	5260 ± 230	>30000	12300 ^b	8780 ± 1280	216 ± 3

^a The CLogP values were calculated from website http://www.syrres.com/esc/est_kowdemo.htm. ^b An accurate estimate of standard error on the IC₅₀ could not be determined due to the poor fit of the curve.

possible differences in the neuroprotective effects of our mercaptoacetamide-based inhibitors relative to the more commonly explored hydroxamates such as TSA or SAHA. In particular, as will be shown below, some of the mercaptoacetamides exhibit a superior neuroprotection profile in an in vitro model of oxidative-stress-induced death.

Results and Discussion

Chemistry. Previously, we have reported on the synthesis of some mercaptoacetamide-based HDAC inhibitors that owe their action to the ability of the thiol and carbonyl groups to interact with the zinc atom present in the catalytic gorge of the HDACs.²⁶ We have also found that some of these compounds

Scheme 1. Synthesis of Mercaptoacetamides **2**, **6**, **7**, and **11–13****Scheme 2.** Synthesis of Hydroxamates **1**, **3**, **4**, **5**, and **8–10**

are very potent in blocking prostate tumor xenograft growth in rodents. As we were aware of the fact that the hydroxamate group is associated with potential toxicity,²⁷ we believed that it was important to compare these two classes of HDAC inhibitors head-to-head for their effects on neurons. Thus, 13 mercaptoacetamides and hydroxamates with CLogP values ranging from 0.78 to 2.86 were chosen from our HDAC inhibitors library, and their structures and inhibitory activities toward HDACs **1**, **2**, **8**, **10**, and **6** are provided in Table 1. The synthetic procedures used for the preparation of the mercaptoacetamides (**2**, **6**, **7**, and **11–13**) from trityl-protected mercaptoacetic acid and its methyl ester are outlined in Scheme 1. Other hydroxamates (**1**, **4**, **5**, and **8–10**) were prepared from their carboxylic acid precursors using general literature methods (Scheme 2).²⁸

HDAC Inhibitors Protect Cortical Neurons from Oxidative Stress-Induced Death. The possible effects of our hydroxamic acid-based or mercaptoacetamide-based HDAC inhibitors were assessed in comparison with the commercially available hydroxamate-based inhibitors, TSA and Scriptaid, using an *in vitro* model of oxidative stress-induced neurodegeneration in primary cortical neurons. In this model, neurodegeneration is induced by the presence of a 5 mM concentration of the glutamate analog, homocysteate (HCA),²⁸ which depletes the cellular antioxidant glutathione by the competitive inhibition of cyst(e)ine uptake at the level of the plasma membrane cystine/glutamate antiporter system xc⁻. Because cysteine is required for synthesis of glutathione, the inhibition of its uptake results

in glutathione depletion. Cellular redox homeostasis, therefore, becomes disrupted with the accumulation of endogenously produced and unopposed oxidants resulting in neuronal degeneration over an approximately 24 hour period of time. Importantly, primary neurons at this early developmental stage lack ionotropic and metabotropic receptors and are not susceptible to excitotoxicity, rather death is induced by accumulation of unopposed free radicals and the neurons exhibit a number of apoptotic features.²⁹ Moreover, the commercially available HDAC inhibitors such as TSA, SAHA, and sodium butyrate have previously been shown to offer protection in this model.³⁰ Here, in addition to TSA, we also include the commercially available HDAC inhibitor, Scriptaid, and the inactive hydroxamate control, Nullscript. Nullscript, which is structurally similar to Scriptaid, lacks sufficient length in the linker region to allow the hydroxamic acid moiety to coordinate the zinc atom at the catalytic core of the HDAC enzyme.

The results of our preliminary neuroprotection studies are shown in Figure 1, where the data are presented as bar graphs of cell survival in the presence and absence of HCA after 48 h, which is well beyond the time for neuronal degeneration in this model to occur (Figure 1). Neuron survival was quantified by the MTT assay, a colorimetric assay in which the amount of yellow MTT (3-[4,5-dimethylthiazol-2-yl]2,5-diphenyltetrazolium bromide, Promega, Madison, WI) is reduced to purple formazan by active mitochondrial reductase enzymes in viable cells. These data demonstrate that the most effective neuropro-

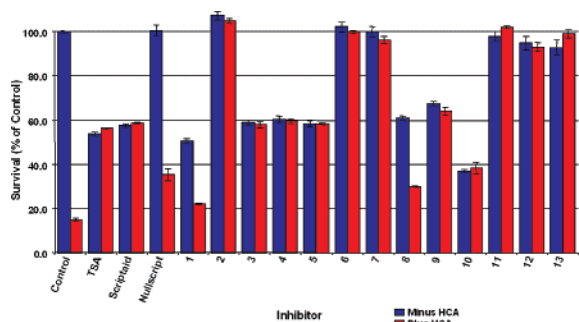


Figure 1. Survival of cortical neurons upon exposure to various HDAC inhibitors in the absence (blue bar) or presence (red bar) of HCA. Data are presented as percent of control \pm SEM.

tection is provided by the mercaptoacetamide-based inhibitors, which protected the cortical neurons to approximately untreated control levels. While many of the hydroxamates exhibit protection against the HCA-induced oxidative stress, in all cases, the inhibitors themselves, at the 10 μ M concentrations used, displayed toxicity. Thus, compared to control cells with no inhibitor present, the viability of the hydroxamate-HDAC inhibitor-treated cells is less. Consistent with Nullscript lacking sufficient length in the linker region to allow HDAC inhibition, it had little protective effect. However, it is interesting to note that unlike the other hydroxamates, Nullscript by itself resulted in no death to the cortical neurons, suggesting that the hydroxamate group is not inherently toxic.

Additionally, we present cell micrographs for the control and HCA-treated cells together with the micrographs for TSA-, hydroxamate **1**-, and mercaptoacetamide **2**-treated cells (Figure 2). The cells were visualized using a two-color fluorescence live–dead assay (Molecular Probes, Eugene, OR). Two-color fluorescence live–dead staining was generated by incubating unfixed cells for 20 min at 37 $^{\circ}$ C with a solution of acetoxy-methyl ester calcein (2 M) and ethidium homodimer-1 (1 M). Calcein acetoxy-methyl ester is hydrolyzed by esterase activity in living cells to membrane-impermeant calcein (green fluorescence), while the ethidium homodimer-1 binds to the nucleic acids of damaged and dead cells (red fluorescence). Again, these cell micrographs show a striking difference between the hydroxamate- and the mercaptoacetamide-based HDAC inhibitors.

To obtain a more precise picture of the effects of HDAC inhibitor concentration on the extent of neuroprotection in the HCA model, dose response curves were obtained for eight of the compounds reported herein. These are displayed in Figure 3. As is apparent, the hydroxamates show approximate bell-

shaped curves when tested in the presence of HCA for 24 h, with the greatest protection being observed at approximately 1 μ M. At concentrations of 10 μ M and above, the toxicity from the hydroxamate-based HDAC inhibitors themselves mask much of the beneficial effect that the HDAC inhibitors may have against oxidative stress. In contrast, the mercaptoacetamides **6** and **13** cause no toxicity at any of the concentrations tested and show a steadily increasing concentration-dependent ability to protect from HCA toxicity, with 100% protection beginning at approximately 10 μ M. Similarly, the mercaptoacetamides **2** and **7** are not toxic and protect against oxidative stress at 10 μ M. However, unlike mercaptoacetamide **6** and **13**, at higher concentrations, these inhibitors do exhibit some toxicity. It is also possible that the greater toxicity of the hydroxamate HDAC inhibitors compared to the mercaptoacetamide inhibitors reflects some isoform specificity for HDAC1. As is apparent from the data presented in Table 1, the hydroxamates all generally exhibit good inhibition for HDAC1. Based on a recent publication investigating the role of HDACs in cerebella granule neurons, in which HDAC1 was found to be essential for survival,³¹ it is possible that the inhibition of HDAC1 could result in neuronal toxicity in this model. Again, this underscores the need to move from pan-HDAC inhibitors such as TSA or Scriptaid to isoform-specific HDAC inhibitors when considering neuroprotective therapies. In contrast to the hydroxamate-based HDAC inhibitors, the mercaptoacetamide-HDAC inhibitors, like compound **13**, show some degree of HDAC6 selectivity. Concurrent with this selectivity is the ability of these inhibitors to protect neurons from oxidative stress-induced death without any inhibitor-associated toxicity. It is possible that some of this protection in the mercaptoacetamide-based inhibitors may, at least in part, be due to radical trapping by the sulfur group. However, our observation that phenylethanethiol, a simple thiol-containing compound that, much like the inactive hydroxamate Nullscript, we would predict to be ineffective at inhibiting HDAC activity, is only protective at high concentrations $>$ 500 μ M (Figure 3), which argues that we are well below the concentration required for a simple antioxidant effect. Indeed, thiol antioxidants that show therapeutic efficacy in this model, such as lipoic acid and *N*-acetylcysteine, are used at concentrations of 100 μ M–1 mM, while doses lower than 100 μ M do not protect.³² Nonetheless, the idea of a bifunctional compound that could both inhibit HDAC activity and have antioxidant activity would hold significant appeal in the clinical setting.

Acetylation of Histone Protein Accompanies HDAC Inhibition. To investigate whether the neuroprotective concentrations of the HDAC inhibitors used result in global histone acetylation in neurons and, thus, potentially, changes in gene

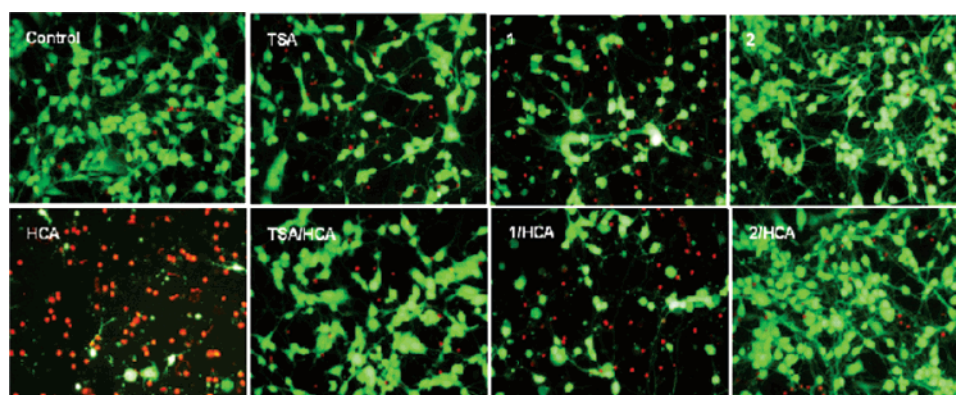


Figure 2. Cell micrographs of cortical neurons treated with HDAC inhibitor in the presence or absence of HCA. The cells were visualized using a two-color fluorescence live–dead assay (Molecular Probes, Eugene, OR).

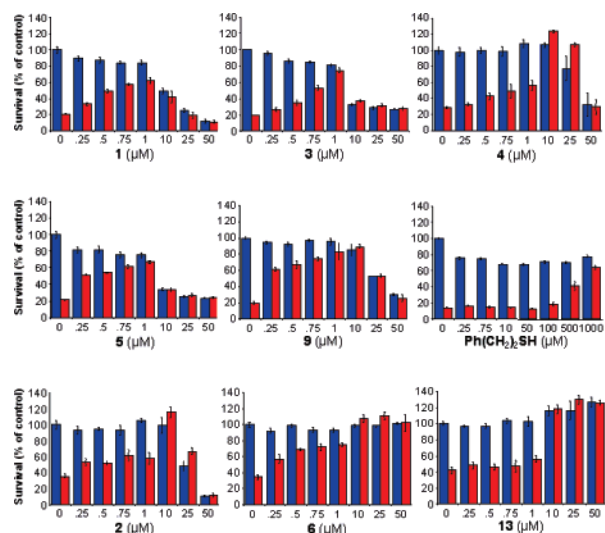


Figure 3. Dose-dependent neuroprotection for eight of the HDAC inhibitors and phenylethanethiol in the HCA-cortical neuron model.

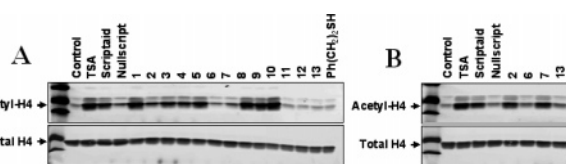


Figure 4. Acetylation levels of histone H4 after treatment with some of the HDAC inhibitors. (A) Effect of different HDAC inhibitors at 10 μM . (B) Effect of different HDAC inhibitors at 50 μM .

transcription, the relative acetylation levels of histone H4 were evaluated after treatment with the HDAC inhibitor compounds (Figure 4A). Histone proteins were acid-precipitated from cell nuclear extracts obtained from rat primary cortical neurons treated with TSA, Scriptaid, Nullscript, and the new ligands at 10 μM for 8 h. Western blot analysis using acetyl-histone H4-specific antibodies (Upstate Cell Signaling Solutions, Charlottesville, VA) demonstrates that acetylation of H4 histone proteins is promoted by some but not all of the HDAC inhibitors. It is, therefore, clear that the extent of H4 acetylation does not correlate with the degree of cellular protection. In fact, for the most part, there is a good correlation between the level of H4 acetylation and neuronal toxicity. Because some of the mercaptoacetamide-based HDAC inhibitors showed toxicity at higher concentrations, we examined whether this toxicity was reflected by histone H4 acetylation. Histone proteins were acid-precipitated from cell nuclear extracts obtained from rat primary cortical neurons treated with several different mercaptoacetamide-based inhibitors at 50 μM for 8 h. Immunoblot analysis of acetyl-H4 demonstrated that with the mercaptoacetamides that showed toxicity at this concentration (compounds **2** and **7**), there was a marked increase in H4 acetylation, whereas inhibitors that showed no toxicity at this concentration (compounds **6** and **13**) induced no increased H4 acetylation (Figure 4B). These findings suggest that the HDAC or HDACs that are the target for neuroprotection against oxidative stress do not play a predominant role in global transcription in the nucleus. This result would also be consistent with our findings that toxicity correlated with the ability of our ligands, particularly the hydroxamates, to inhibit HDAC1 and HDAC2. As previously discussed, HDAC1 activity has been shown to be required for neuronal survival. The mechanism of this survival has been shown to be through histone deacetylation and suppression of the c-Jun promoter within the nucleus.³¹ Thus, the loss of

repression at this promoter by inhibiting HDAC1 would result in increased levels of the pro-apoptotic c-Jun and neuronal death. Although further work is required to understand these differences, including more extensive studies of isozyme selectivity, our results are consistent with the possibility that the mercaptoacetamide-based HDAC inhibitors interact with a different subset of the HDAC isozymes, or alternatively, are interacting selectively with only the cytoplasmic HDACs that are crucial for protection from oxidative stress. Further experiments are underway to investigate these and other putative mechanisms of mercaptoacetamide-based HDAC inhibitor neuroprotection.

Summary

The present research findings suggest that it will be important to take into consideration the nature of the ZBG that is present in the HDAC inhibitors that are being used to accomplish specific therapeutic endpoints. We note that the dose-dependent toxicity associated with the hydroxamate-based inhibitors is likely due to the inhibition of pro-survival or the activation of pro-death or toxic (in a neuronal context) gene(s) rather than the hydroxamate group per se. As in our experiments, we see no toxicity using the hydroxamate-containing HDAC inhibitor control, Nullscript. Thus, in treating neurodegenerative diseases, some of the mercaptoacetamide-based inhibitors may prove worthy of further consideration, although ultimately, it will be necessary to carefully assess these inhibitors in other models of neurodegeneration in their ability to penetrate to the blood–brain barrier and for any other toxicological or metabolic liabilities they might have. Nonetheless, we believe these findings are significant, for they chart a possible course forward in the development of HDAC inhibitor-based therapies for neurodegenerative disorders. The isoform data presented for the compounds disclosed herein, while still incomplete, are in fact more thorough than the data generally available in the literature. These data thus provide structural information relevant to identifying more selective molecules. Efforts are also being made to obtain measurements of IC₅₀ values against the missing HDAC isoforms, which will be reported in due course.

Experimental Section

Chemistry. ¹H NMR and ¹³C NMR spectra were recorded on Bruker spectrometer at 300/400 MHz and 75/100 MHz, respectively, with TMS as an internal standard. HRMS experiment was performed on Q-TOF-2TM (Micromass). TLC was performed with Merck 60F₂₅₄ silica gel plates. Preparative TLC was performed with analtech 1000 mm silica gel GF plates. Column chromatography was performed using Merck silica gel (40–60 mesh). HPLC was carried out on an ACE AQ column (100 × 4.6 mm and 250 × 10 mm), with detection at 210, 240, 254, 280, and 300 nm on a Shimadzu SPD-10A VP detector; flow rate = 2.0–3.5 mL/min; from 10% acetonitrile in water to 100% acetonitrile with 0.05% TFA. Detailed methods for preparation of intermediates **14**–**27** can be found in the Supporting Information together with their HPLC data and conditions for the tested compounds.

General Procedure for the Synthesis of Mercaptoacetamides by Trityl Group Deprotection. To a solution or suspension of compound **14** (1 mmol) in dichloromethane (10 mL) was added trifluoroacetic acid (1.0 mL), followed by the addition of triethylsilane (1.1 mmol). After the mixture was stirred at room temperature for 2 h, saturated sodium bicarbonate (15 mL) was added slowly, and the mixture was stirred for 30 min. The organic layer was separated, and the aqueous layer was extracted with chloroform several times (followed by TLC). The combined organic layers were dried over sodium sulfate and concentrated in vacuo. The crude product was purified by column chromatography to give mercaptoacetamides **2** (248 mg, 75%).

6-(2-Mercaptoacetyl-amino)-hexanoic Acid Quinolin-8-yl-amide (2). ^1H NMR (CDCl_3 , 300 MHz) δ (ppm) 9.81 (br s, 1H), 8.80 (dd, $J = 4.2$, 1.5 Hz, 1H), 8.77 (dd, $J = 6.9$ and 1.8 Hz, 1H), 8.16 (dd, $J = 8.4$ and 1.5 Hz, 1H), 7.56–7.43 (m, 3H), 6.81 (br s, 1H), 3.32 (dt, $J = 6.6$ and 6.3 Hz, 2H), 3.21 (d, $J = 9.0$ Hz, 2H), 2.58 (t, $J = 7.2$ Hz, 2H), 1.90 (t, $J = 9.0$ Hz, 1H), 1.85 (m, 2H), 1.62 (m, 2H), 1.48 (m, 2H). ^{13}C NMR (CDCl_3 , 75 MHz) δ (ppm) 171.5, 169.1, 148.2, 138.3, 136.4, 134.4, 127.9, 127.4, 121.6, 121.5, 116.4, 39.6, 37.8, 29.1, 28.3, 26.4, 25.0. ESI-HRMS calcd for $[\text{C}_{17}\text{H}_{21}\text{N}_3\text{O}_2\text{S} + \text{H}]^+$, 332.1432; found, 332.1429.

2-Mercapto-N-[6-(3-phenyl-ureido)-hexyl]acetamide (6, Yield 78%). ^1H NMR ($\text{DMSO-}d_6$, 300 MHz) δ (ppm) 8.37 (br s, 1H), 7.97 (br t, $J = 5.1$ Hz, 1H), 7.37 (d, $J = 7.5$ Hz, 2H), 7.20 (t, $J = 7.5$ Hz, 2H), 6.87 (t, $J = 7.5$ Hz, 1H), 6.10 (br t, $J = 5.4$ Hz, 1H), 3.07 (d, $J = 7.8$ Hz, 2H), 3.04 (t, $J = 6.9$ Hz, 2H), 2.71 (t, $J = 7.8$ Hz, 1H), 1.41 (m, 4H), 1.28 (m, 4H). ^{13}C NMR ($\text{DMSO-}d_6$, 75 MHz) δ (ppm) 169.4, 155.2, 140.6, 128.6, 120.9, 117.5, 38.96, 38.79, 29.7, 29.0, 27.1, 26.1 (2C). ESI-HRMS calcd for $[\text{C}_{15}\text{H}_{23}\text{N}_3\text{O}_2\text{S} + \text{Na}]^+$, 332.1409; found, 332.1407.

4-Dimethylamino-N-[6-(2-mercaptoacetyl-amino)hexyl]benzamide (7, Yield 91%). ^1H NMR (CDCl_3 , 300 MHz) δ (ppm) 7.68 (d, $J = 9.0$ Hz, 2H), 6.89 (br s, 1H), 6.66 (d, $J = 9.0$ Hz, 2H), 6.18 (br t, 1H), 3.43 (dt, $J = 6.9$ and 6.0 Hz, 2H), 3.27 (dt, $J = 6.6$ and 6.0 Hz, 2H), 3.24 (d, $J = 9.0$ Hz, 2H), 3.01 (s, 6H), 1.94 (t, $J = 9.0$ Hz, 1H), 1.60 (m, 2H), 1.54 (m, 2H), 1.39 (m, 4H). ^{13}C NMR (CDCl_3 , 75 MHz) δ (ppm) 169.3, 167.6, 152.4, 128.3, 121.4, 111.1, 40.1, 39.4, 39.3, 29.7, 29.2, 28.3, 26.1, 26.0. ESI-HRMS calcd for $[\text{C}_{17}\text{H}_{27}\text{N}_3\text{O}_2\text{S} + \text{Na}]^+$, 360.1722; found, 360.1721.

4-Dimethylamino-N-[5-(2-mercaptoacetyl-amino)pentyl]benzamide (11, Yield 86%). ^1H NMR (CDCl_3 , 300 MHz) δ (ppm) 7.68 (d, $J = 9.0$ Hz, 2H), 6.88 (br s, 1H), 6.66 (d, $J = 9.0$ Hz, 2H), 6.19 (br t, 1H), 3.44 (dt, $J = 6.9$, 6.0 Hz, 2H), 3.29 (dt, $J = 6.6$, 6.0 Hz, 2H), 3.20 (d, $J = 9.0$ Hz, 2H), 3.02 (s, 6H), 1.90 (t, $J = 9.0$ Hz, 1H), 1.61 (m, 4H), 1.41 (m, 2H). ^{13}C NMR (CDCl_3 , 75 MHz) δ (ppm) 169.5, 167.7, 152.4, 128.3, 121.2, 111.1, 40.1, 39.6, 39.2, 29.4, 28.7, 28.3, 23.7. ESI-HRMS calcd for $[\text{C}_{16}\text{H}_{25}\text{N}_3\text{O}_2\text{S} + \text{Na}]^+$, 346.1565; found, 346.1559.

4-Dimethylamino-N-[4-(2-mercaptoacetyl-amino)butyl]benzamide (12, Yield 84%). ^1H NMR (CDCl_3 , 300 MHz) δ (ppm) 7.69 (d, $J = 9.0$ Hz, 2H), 7.05 (br s, 1H), 6.66 (d, $J = 9.0$ Hz, 2H), 6.31 (br s, 1H), 3.47 (dt, $J = 6.3$ and 6.3 Hz, 2H), 3.33 (dt, $J = 6.6$ and 6.0 Hz, 2H), 3.24 (d, $J = 8.7$ Hz, 2H), 3.02 (s, 6H), 1.94 (t, $J = 8.7$ Hz, 1H), 1.64 (m, 4H). ^{13}C NMR (CDCl_3 , 75 MHz) δ (ppm) 169.7, 167.7, 152.4, 128.4, 121.1, 111.0, 40.1, 39.5, 39.3, 28.3, 27.2, 26.6. ESI-HRMS calcd for $[\text{C}_{15}\text{H}_{23}\text{N}_3\text{O}_2\text{S} + \text{Na}]^+$, 332.1409; found, 332.1404.

4-Dimethylamino-N-[3-(2-mercaptoacetyl-amino)propyl]benzamide (13, Yield 93%). ^1H NMR (CDCl_3 , 300 MHz) δ (ppm) 7.74 (d, $J = 9.0$ Hz, 2H), 7.37 (br t, 1H), 6.85 (br t, 1H), 6.68 (d, $J = 9.0$ Hz, 2H), 3.48 (dt, $J = 6.3$ and 6.0 Hz, 2H), 3.38 (dt, $J = 6.3$ and 6.0 Hz, 2H), 3.25 (d, $J = 9.0$ Hz, 2H), 3.02 (s, 6H), 1.96 (t, $J = 9.0$ Hz, 1H), 1.74 (m, 2H). ^{13}C NMR (CDCl_3 , 75 MHz) δ (ppm) 170.3, 168.4, 152.4, 128.4, 121.0, 111.1, 40.2, 36.4, 36.0, 29.8, 28.5. ESI-HRMS calcd for $[\text{C}_{14}\text{H}_{21}\text{N}_3\text{O}_2\text{S} + \text{Na}]^+$, 318.1252; found, 318.1248.

General Synthesis of Hydroxamate by Hydrogenation. A suspension of the *O*-benzyl-protected compound (**26**; 0.031 g, 0.049 mmol) and 10% Pd/C (0.010 g) in methanol (5 mL) was stirred under a hydrogen atmosphere at rt for 4 h. The catalyst was removed by filtration through a pad of Celite, and the residue was thoroughly washed with MeOH. The solvent was evaporated in vacuo, and the residue was crystallized from methanol/ether, 5:95, to give hydroxamate **8** (0.008 g, 30%).

Octanedioic Acid {2'-[2-Amino-3-(1*H*-indol-3-yl)propionyl-amino]biphenyl-4-yl}amide Hydroxyamide (8). ^1H NMR (CD_3OD , 300 MHz) δ (ppm) 7.74 (d, $J = 7.7$ Hz, 1H), 7.67–7.52 (m, 3H), 7.48–7.23 (m, 5H), 7.22–7.09 (m, 4H), 7.08–6.96 (m, 1H), 4.05–3.96 (m, 1H), 3.35–3.25 (m, 1H), 3.15–3.02 (m, 1H), 2.37 (d, $J = 7.0$ Hz, 2H), 2.10 (d, $J = 7.0$ Hz, 2H), 1.78–1.30 (m, 8H). ^{13}C NMR ($\text{DMSO-}d_6$, 75 MHz) δ (ppm) 173.1, 171.3, 167.5, 137.5, 136.4, 136.0, 133.8, 132.7, 129.8, 128.7, 127.2, 126.4, 126.1, 125.2,

123.8, 121.2, 119.8, 118.6, 117.4, 114.7, 110.9, 106.1, 99.5, 53.5, 36.0, 31.9, 28.1, 28.0, 26.9, 24.9, 24.8. ESI-HRMS calcd for $[\text{C}_{31}\text{H}_{35}\text{N}_5\text{O}_4 + \text{H}]^+$, 542.2761; found, 542.2762.

Octanedioic Acid [2'-(2-Amino-3-phenylpropionyl-amino)-biphenyl-4-yl]amide hydroxyamide (1, Yield 90%). ^1H NMR ($\text{DMSO-}d_6$, 400 MHz) δ (ppm) 10.34 (s, 1H), 9.96 (s, 1H), 8.66 (br s, 1H), 8.22 (d, $J = 8.1$ Hz, 1H), 7.64 (d, $J = 8.4$ Hz, 2H), 7.35–7.14 (m, 10 H), 3.52 (m, 1H), 3.34 (m, 2H), 3.01 (dd, $J = 4.0$ and 13.0 Hz, 1H), 2.75 (dd, $J = 8$ and 13 Hz, 1H), 2.31 (t, $J = 7.0$ Hz, 2H), 1.94 (t, $J = 7.0$ Hz, 2H), 1.59 (m, 2H), 1.49 (m, 2H), 1.23 (m, 4H). ^{13}C NMR ($\text{DMSO-}d_6$, 100 MHz) δ (ppm) 173.1, 171.7, 169.5, 139.2, 138.6, 135.2, 132.6, 132.5, 130.6, 129.8, 129.7, 128.1, 126.7, 124.5, 121.5, 119.5, 55.9, 36.8, 32.7, 28.8, 25.4. ESI-HRMS calcd for $[\text{C}_{29}\text{H}_{34}\text{N}_4\text{O}_4 + \text{H}]^+$, 503.2658; found, 503.2648.

Octanedioic Acid {2'-[2-Amino-3-(4-hydroxy-phenyl)propionyl-amino]biphenyl-4-yl}amide Hydroxyamide (9, Yield 52%). ^1H NMR (CD_3OD , 300 MHz) δ (ppm) 7.90 (d, $J = 7.8$ Hz, 1H), 7.61 (d, $J = 8.2$ Hz, 2H), 7.40–7.10 (m, 6H), 7.02 (d, $J = 7.2$ Hz, 2H), 6.74 (d, $J = 8.2$ Hz, 2H), 3.65 (t, $J = 5.8$ Hz, 1H), 3.00–2.90 (m, 1H), 2.82–2.70 (m, 1H), 2.39 (t, $J = 7.1$ Hz, 2H), 2.11 (t, $J = 7.1$ Hz, 2H), 1.75–1.30 (m, 8H). ^{13}C NMR (CD_3OD , 75 MHz) δ (ppm) 173.7, 173.2, 171.9, 156.5, 138.4, 135.1, 134.3, 134.3, 130.5, 130.4, 129.6, 127.9, 127.5, 123.9, 115.5, 120.3, 56.6, 39.2, 36.8, 32.7, 28.9, 28.8, 25.9, 25.7, 15.7. ESI-HRMS calcd for $[\text{C}_{29}\text{H}_{34}\text{N}_4\text{O}_5 + \text{H}]^+$, 519.2602; found, 519.2595.

6-(3-Adamantan-1-yl-ureido)hexanoic Acid Hydroxyamide (3, Yield 72%). ^1H NMR (CD_3OD , 300 MHz) δ (ppm) 3.04 (t, $J = 7.2$ Hz, 2H), 2.09 (t, $J = 7.5$ Hz, 2H), 2.03 (m, 3H), 1.96 (m, 6H), 1.70 (m, 6H), 1.62 (m, 2H), 1.45 (m, 2H), 1.34 (m, 2H). ^{13}C NMR (CD_3OD , 75 MHz) δ (ppm) 173.0, 160.5, 51.5, 43.6, 40.5, 37.7, 33.8, 31.19, 31.14, 27.5, 26.6. ESI-HRMS calcd for $[\text{C}_{17}\text{H}_{29}\text{N}_3\text{O}_3\text{S} + \text{Na}]^+$, 346.2106; found, 346.2098.

8-[3-(4-Dimethylaminobenzyl)ureido]octanoic Acid Hydroxyamide (4, Yield 41%). ^1H NMR ($\text{DMSO-}d_6$, 300 MHz) δ (ppm) 10.33 (br s, 1H), 8.66 (br s, 1H), 7.05 (d, $J = 8.4$ Hz, 2H), 6.67 (d, $J = 8.4$ Hz, 2H), 6.05 (t, $J = 5.7$ Hz, 1H), 5.81 (t, $J = 5.7$ Hz, 1H), 4.05 (d, $J = 6.0$ Hz, 2H), 2.97 (dt, $J = 6.6$ and 6.0 Hz, 2H), 2.85 (s, 6H), 1.93 (t, $J = 7.5$ Hz, 2H), 1.47 (m, 2H), 1.34 (m, 2H), 1.24 (m, 6H). ^{13}C NMR ($\text{DMSO-}d_6$, 75 MHz) δ (ppm) 169.1, 158.0, 149.5, 128.4, 128.0, 112.4, 42.5, 40.4, 39.2, 32.3, 30.0, 28.59, 28.51, 26.3, 25.1. ESI-HRMS calcd for $[\text{C}_{18}\text{H}_{30}\text{N}_4\text{O}_3 + \text{Na}]^+$, 373.2215; found, 373.2198.

7-[3-(4-Dimethylaminophenyl)ureido]heptanoic Acid Hydroxyamide (5, Yield 34%). ^1H NMR ($\text{DMSO-}d_6$, 300 MHz) δ (ppm) 10.34 (br s, 1H), 8.64 (br s, 1H), 7.98 (br s, 1H), 7.17 (d, $J = 9.0$ Hz, 2H), 6.65 (d, $J = 9.0$ Hz, 2H), 5.91 (t, $J = 5.7$ Hz, 1H), 3.03 (dt, $J = 6.6$ and 6.0 Hz, 2H), 2.79 (s, 6H), 1.94 (t, $J = 7.5$ Hz, 2H), 1.48 (m, 2H), 1.39 (m, 2H), 1.25 (m, 4H). ^{13}C NMR ($\text{DMSO-}d_6$, 75 MHz) δ (ppm) 169.1, 155.6, 145.9, 130.7, 119.6, 113.3, 40.9, 39.0, 32.2, 29.8, 28.4, 26.2, 25.1. ESI-HRMS calcd for $[\text{C}_{16}\text{H}_{26}\text{N}_4\text{O}_3 + \text{H}]^+$, 323.2083; found, 323.2088.

Synthesis of Hydroxamate through the Mixed Anhydride. To a solution of acid **23** (0.100 g, 0.26 mmol) in dry THF was added Et_3N (0.18 mL, 1.3 mmol) under nitrogen, and the solution was stirred for 5 min. The solution was cooled to -15 °C and stirred for another 5 min. Then *iso*-butyl chloroformate (67 μL , 0.52 mmol) was added dropwise, and the mixture was stirred for 15 min. The solid was filtered off. The filtrate was cooled to 0 °C, and a 50% aqueous solution (1 mL) of NH_2OH was added over 10 min. The reaction mixture was diluted with EtOAc, washed with saturated aqueous NH_4Cl and brine, and then dried over Na_2SO_4 . The solvent was removed by rotary evaporation. The crude solid was purified by HPLC to give compound **10** (0.027 g, 26.4%).

Octanedioic Acid Hydroxyamide [4-(3-Nitro-phenyl)thiazol-2-yl]amide (10). ^1H NMR ($\text{DMSO-}d_6$, 300 MHz) δ (ppm) 12.3 (s, 1H), 10.3 (s, 1H), 8.72 (s, 1H), 8.67 (br s, 1H), 8.34 (d, $J = 7.7$ Hz, 1H), 8.17 (dd, $J = 8.1$ and 1.5 Hz, 1H), 7.91 (s, 1H), 7.73 (t, $J = 7.9$ Hz, 1H), 2.45 (t, $J = 7.2$ Hz, 2H), 1.94 (t, $J = 7.2$ Hz, 2H), 1.60 (br s, 2H), 1.50–1.35 (m, 4H), 1.50 (t, $J = 6.1$ Hz, 2H). ^{13}C NMR ($\text{DMSO-}d_6$, 100 MHz) δ (ppm) 172.1, 169.5, 158.8, 148.7, 146.7, 136.2, 132.1, 130.8, 122.7, 120.4, 110.8, 35.3, 32.6

28.7, 25.4, 24.9. ESI-HRMS calcd for $[C_{17}H_{20}N_4O_5S + H]^+$, 393.1227; found, 393.1227.

Biological Methods. HDAC Inhibition Assay. The inhibitory effects of compounds on HDAC activity were determined using a fluorescence-based assay with electrophoretic separation of substrate and product carried out using a microfluidic system followed by quantitation of fluorescence intensity in the substrate and product peaks. The assays were performed using isolated HDAC isoforms that had been expressed as 6 × His-tagged fusion proteins in a baculovirus expression system in Sf9 cells. HDACs 1, 2, 3, 6, and 8 were expressed as full length fusion proteins. The HDAC10 fusion protein was expressed as a carboxy-terminal deletion of 38 amino acids (residues 632–669). HDAC3 was coexpressed with a fragment of the SMRT gene (residues 395–489) to generate enzymatically active protein. Purified proteins were incubated with 1 μM carboxyfluorescein (FAM)-labeled acetylated peptide substrate and test compound for 17 h at 25 °C in HDAC assay buffer containing 100 mM HEPES (pH 7.5), 25 mM KCl, 0.1% BSA, and 0.01% Triton X-100. Reactions were terminated by the addition of buffer containing 0.078% SDS for a final SDS concentration of 0.05%. Substrate and product were separated electrophoretically using a Caliper LabChip 3000 system with blue laser excitation and green fluorescence detection (CCD2). The fluorescence intensity in the substrate and product peaks was determined using the Well Analyzer software on the Caliper system. The reactions were performed in duplicate for each sample. IC₅₀ values were automatically calculated using the IDBS XLFit version 4.2.1 plug-in for Microsoft Excel and the XLFit 4 Parameter Logistic Model (sigmoidal dose–response model): $(A + ((B - A)/1 + (C/x)^D))$, where x is compound concentration, A is the estimated minimum, B is the estimated maximum of % inhibition, C is the inflection point, and D is the Hill slope of the sigmoidal curve. The standard errors of the IC₅₀s were automatically calculated using the IDBS XLFit version 4.2.1 plug-in for Microsoft Excel and the formula $xf4_FitResultStdError()$.

Primary Neurons and Cell Culture. Cell cultures were obtained from the cerebral cortex of fetal Sprague–Dawley rats (embryonic day 17), as described previously.²⁹ All experiments were initiated 24 h after plating. Under these conditions, the cells are not susceptible to glutamate-mediated excitotoxicity.

Neuron Viability Assays. For cytotoxicity studies, cells were rinsed with warm PBS and then placed in minimum essential medium (Invitrogen) containing 5.5 g/L glucose, 10% fetal calf serum, 2 mM L-glutamine, and 100 μM cystine. Oxidative stress was induced by the addition of the glutamate analog HCA (5 mM) to the media. HCA was diluted from 100-fold concentrated solutions that were adjusted to pH 7.5. In combination with HCA, TSA (0.66 μM), or Scriptaid (6.13 μM) or Nullscript (6.13 μM), or the novel HDAC inhibitor compounds (10 μM, unless stated differently in the text) were added. Viability was assessed after 48 h by calcein-acetoxymethyl ester (AM)/ethidium homodimer-1 staining (live/dead assay; Molecular Probes, Eugene, OR) under fluorescence microscopy and the MTT assay method. Each bar represents the mean ± SE of four replicates.

Histone Precipitation and Western Blot Analysis. Approximately one million treated neurons were incubated in 1 mL hypotonic lysis buffer containing 10 mM Tris-HCl pH8, 1 mM KCl, 1.5 mM MgCl₂, 1 mM DTT, 1 mM aprotinin, 1 mM pepstatin, and 0.4 mM PMSF for 30 min rotating at 4 °C. Nuclei were pelleted by centrifugation for 10 min at 10 000 rpm, resuspended in 200 μL 0.4 N H₂SO₄ and rotated for 12 h at 4 °C. Following centrifugation at 13 000 rpm for 10 min the supernatant was transferred to a new tube, and the histone proteins were precipitated by adding 66 μL of 100% TCA dropwise followed by a 30 min incubation on ice. Histone proteins were pelleted by centrifugation at 13 000 rpm for 10 min, washed twice with ice-cold acetone, dried at room temperature for 20–40 min, and resuspended in 50 μL H₂O. Twenty microliters of total histone proteins were boiled in Laemmli buffer and electrophoresed under reducing conditions on 15% polyacrylamide gel. Histone proteins were transferred to a nitrocellulose membrane (Bio-Rad). Nonspecific binding was

inhibited by incubation in Tris-buffered saline with Tween 20 (TBST: 50 mM Tris-HCl, pH 8.0, 0.9% NaCl, and 0.1% Tween 20) containing 5% nonfat dried milk for at least 1.5 h. Primary antibodies against acetylated histone H4 or total histone H4 (Upstate) were diluted 1:1000 or 1:4000, respectively, in TBST containing 5% milk and incubated with the membrane for 3 h at room temperature, followed by incubation with anti-rabbit horse-radish peroxidase-conjugated secondary antibodies for 2 h at room temperature. Acetyl histone H4 and total histone H4 immunoreactivity was detected according to the enhanced chemiluminescent protocol (Amersham Biosciences).

Acknowledgment. This work was supported in part by gift money (A.P.K.) and the Goldsmith Foundation (B.L.). We also wish to thank the HighQ Foundation for providing support for the HDAC assays.

Supporting Information Available: Methods for preparation of intermediates 14–27 and the HPLC data of tested compounds. This material is available free of charge via the Internet at <http://pubs.acs.org>.

References

- (1) Marks, P. A.; Dokmanovic, M. Histone deacetylase inhibitors: Discovery and development as anticancer agents. *Expert Opin. Invest. Drugs* **2005**, *14*, 1497–1511.
- (2) Grunstein, M. Histone acetylation in chromatin structure and transcription. *Nature* **1997**, *389*, 349–352.
- (3) Kurdistani, S. K.; Grunstein, M. Histone acetylation and deacetylation in yeast. *Nat. Rev. Mol. Cell Biol.* **2003**, *4*, 276–284.
- (4) Struhl, K.; Moqtaderi, Z. The TAFs in the HAT. *Cell* **1998**, *94*, 1–4.
- (5) Wolffe, A. P.; Guschin, D. Review: Chromatin structural features and targets that regulate transcription. *J. Struct. Biol.* **2000**, *129*, 102–122.
- (6) Marks, P. A.; Richon, V. M.; Rifkind, R. A. Histone deacetylase inhibitors: Inducers of differentiation or apoptosis of transformed cells. *J. Natl. Cancer Inst.* **2000**, *92*, 1210–1216.
- (7) Carducci, M. A.; Gilbert, J.; Bowling, M. K.; Noe, D.; Eisenberger, M. A.; Simibaldi, V.; Zabelina, Y.; Chen, T. L.; Grochow, L. B.; Donehower, R. C. A Phase I clinical and pharmacological evaluation of sodium phenylbutyrate on an 120-h infusion schedule. *Clin. Cancer Res.* **2001**, *7*, 3047–3055.
- (8) Kelly, W. K.; Richon, V. M.; O'Connor, O.; Curley, T.; MacGregor-Curtelli, B.; Tong, W.; Klang, M.; Schwartz, L.; Richardson, S.; Rosa, E.; Drobnyak, M.; Cordon-Cordo, C.; Chia, J. H.; Rifkind, R.; Marks, P. A.; Scher, H. Phase I clinical trial of histone deacetylase inhibitor: Suberoylanilide hydroxamic acid administered intravenously. *Clin. Cancer Res.* **2003**, *9*, 3578–3588.
- (9) Sasakawa, Y.; Naoe, Y.; Inoue, T.; Sasakawa, T.; Matsuo, M.; Manda, T.; Mutoh, S. Effects of FK228, a novel histone deacetylase inhibitor, on human lymphoma U-937 cells in vitro and in vivo. *Biochem. Pharmacol.* **2002**, *64*, 1079–1090.
- (10) Marks, P.; Rifkind, R. A.; Richon, V. M.; Breslow, R.; Miller, T.; Kelly, W. K. Histone deacetylases and cancer: Causes and therapies. *Nat. Rev. Cancer* **2001**, *1*, 194–202.
- (11) Marks, P. A.; Richon, V. M.; Miller, T.; Kelly, W. K. Histone deacetylase inhibitors. *Adv. Cancer Res.* **2004**, *91*, 137–168.
- (12) Endres, M.; Meisel, A.; Biniszkiwicz, D.; Namura, S.; Prass, K.; Ruscher, K.; Lipski, A.; Jaenisch, R.; Moskowitz, M. A.; Dirnagl, U. DNA methyltransferase contributes to delayed ischemic brain injury. *J. Neurosci.* **2000**, *20*, 3175–3181.
- (13) Qi, X.; Hosoi, T.; Okuma, Y.; Kaneko, M.; Nomura, Y. Sodium 4-phenylbutyrate protects against cerebral ischemic injury. *Mol. Pharmacol.* **2004**, *66*, 899–908.
- (14) Ren, M.; Leng, Y.; Jeong, M.; Leeds, P. R.; Chuang, D. M. Valproic acid reduces brain damage induced by transient focal cerebral ischemia in rats: Potential roles of histone deacetylase inhibition and heat shock protein induction. *J. Neurochem.* **2004**, *89*, 1358–1367.
- (15) Camelo, S.; Iglesias, A. H.; Hwang, D.; Due, B.; Ryu, H.; Smith, K.; Gray, S. G.; Imitola, J.; Duran, G.; Assaf, B.; Langley, B.; Khoury, S. J.; Stephanopoulos, G.; De Girolami, U.; Ratan, R. R.; Ferrante, R. J.; Dangond, F. Transcriptional therapy with the histone deacetylase inhibitor trichostatin A ameliorates experimental autoimmune encephalomyelitis. *J. Neuroimmunol.* **2005**, *164*, 10–21.
- (16) Ferrante, R. J.; Kubilus, J. K.; Lee, J.; Ryu, H.; Beesen, A.; Zucker, B.; Smith, K.; Kowall, N. W.; Ratan, R. R.; Luthi-Carter, R.; Hersch, S. M. Histone deacetylase inhibition by sodium butyrate chemotherapy ameliorates the neurodegenerative phenotype in Huntington's disease mice. *J. Neurosci.* **2003**, *23*, 9418–9427.

- (17) Hockly, E.; Richon, V. M.; Woodman, B.; Smith, D. L.; Zhou, X.; Rosa, E.; Sathasivam, K.; Ghazi-Noori, S.; Mahal, A.; Lowden, P. A.; Steffan, J. S.; Marsh, J. L.; Thompson, L. M.; Lewis, C. M.; Marks, P. A.; Bates, G. P. Suberoylanilide hydroxamic acid, a histone deacetylase inhibitor, ameliorates motor deficits in a mouse model of Huntington's disease. *Proc. Natl. Acad. Sci. U.S.A.* **2003**, *100*, 2041–2046.
- (18) McCampbell, A.; Taye, A. A.; Whitty, L.; Penney, E.; Steffan, J. S.; Fischbeck, K. H. Histone deacetylase inhibitors reduce polyglutamine toxicity. *Proc. Natl. Acad. Sci. U.S.A.* **2001**, *98*, 15179–15184.
- (19) Steffan, J. S.; Bodai, L.; Pallos, J.; Poelman, M.; McCampbell, A.; Apostol, B. L.; Kazantsev, A.; Schmidt, E.; Zhu, Y. Z.; Greenwald, M.; Kurokawa, R.; Housman, D. E.; Jackson, G. R.; Marsh, J. L.; Thompson, L. M. Histone deacetylase inhibitors arrest polyglutamine-dependent neurodegeneration in *Drosophila*. *Nature* **2001**, *413*, 739–743.
- (20) Gardian, G.; Browne, S. E.; Choi, D. K.; Klivenyi, P.; Gregorio, J.; Kubilus, J. K.; Ryu, H.; Langley, B.; Ratan, R. R.; Ferrante, R. J.; Beal, M. F. Neuroprotective effects of phenylbutyrate in the N171–82Q transgenic mouse model of Huntington's disease. *J. Biol. Chem.* **2005**, *280*, 556–563.
- (21) Minamiyama, M.; Katsuno, M.; Adachi, H.; Waza, M.; Sang, C.; Kobayashi, Y.; Tanaka, F.; Doyu, M.; Inukai, A.; Sobue, G. Sodium butyrate ameliorates phenotypic expression in a transgenic mouse model of spinal and bulbar muscular atrophy. *Hum. Mol. Genet.* **2004**, *13*, 1183–1192.
- (22) Tsankova, N. M.; Berton, O.; Renthal, W.; Kumar, A.; Neve, R. L.; Nestler, E. J. Sustained hippocampal chromatin regulation in a mouse model of depression and antidepressant action. *Nat. Neurosci.* **2006**, *9*, 519–525.
- (23) Gantt, S. L.; Gattis, S. G.; Fierke, C. A. Catalytic activity and inhibition of human histone deacetylase 8 is dependent on the identity of the active site metal ion. *Biochemistry* **2006**, *45*, 6170–6178.
- (24) Hu, E.; Dul, E.; Sung, C. M.; Chen, Z.; Kirkpatrick, R.; Zhang, G. F.; Johanson, K.; Liu, R.; Lago, A.; Hofmann, G.; Macarron, R.; de los Frailes, M.; Perez, P.; Krawiec, J.; Winkler, J.; Jaye, M. Identification of novel isoform-selective inhibitors within class I histone deacetylases. *J. Pharmacol. Exp. Ther.* **2003**, *307*, 720–728.
- (25) Gregoretti, I. V.; Lee, Y. M.; Goodson, H. V. Molecular evolution of the histone deacetylase family: Functional implications of phylogenetic analysis. *J. Mol. Biol.* **2004**, *338*, 17–31.
- (26) Chen, B.; Petukhov, P. A.; Jung, M.; Velena, A.; Eliseeva, E.; Dritschilo, A.; Kozikowski, A. P. Chemistry and biology of mercaptoacetamides as novel histone deacetylase inhibitors. *Bioorg. Med. Chem. Lett.* **2005**, *15*, 1389–1392.
- (27) Kruger, A.; Soeltl, R.; Sopov, I.; Kopitz, C.; Arlt, M.; Magdolen, V.; Harbeck, N.; Gansbacher, B.; Schmitt, M. Hydroxamate-type matrix metalloproteinase inhibitor batimastat promotes liver metastasis. *Cancer Res.* **2001**, *61*, 1272–1275.
- (28) Wittich, S.; Scherf, H.; Xie, C.; Brosch, G.; Loidl, P.; Gerhäuser, C.; Jung, M. Structure–activity relationships on phenylalanine-containing inhibitors of histone deacetylase: in vitro enzyme inhibition, induction of differentiation, and inhibition of proliferation in friend leukemic cells. *J. Med. Chem.* **2002**, *45*, 3296–3309.
- (29) Ratan, R. R.; Murphy, T. H.; Baraban, J. M. Oxidative stress induces apoptosis in embryonic cortical neurons. *J. Neurochem.* **1994**, *62*, 376–379.
- (30) Ryu, H.; Lee, J.; Olofsson, B. A.; Mwidau, A.; Dedeoglu, A.; Escudero, M.; Flemington, E.; Azizkhan-Clifford, J.; Ferrante, R. J.; Ratan, R. R. Histone deacetylase inhibitors prevent oxidative neuronal death independent of expanded polyglutamine repeats via an Sp1-dependent pathway. *Proc. Natl. Acad. Sci. U.S.A.* **2003**, *100*, 4281–4286.
- (31) Morrison, B. E.; Majdzadeh, N.; Zhang, X.; Lyles, A.; Bassel-Duby, R.; Olson, E. N.; D'Mello, S. R. Neuroprotection by histone deacetylase-related protein. *Mol. Cell. Biol.* **2006**, *26*, 3550–3564.
- (32) Han, D.; Sen, C. K.; Roy, S.; Kobayashi, M. S.; Tritschler, H. J.; Packer, L. Protection against glutamate-induced cytotoxicity in C6 glial cells by thiol antioxidants. *Am. J. Physiol.* **1997**, *273*, R1771–R1778.

JM070178X